AD-A039 263 AEROSPACE CORP EL SEGUNDO CALIF AEROPHYSICS LAB F/G 7/2
COLLISIONAL QUENCHING AND RADIATIVE DECAY STUDIES OF NF(A1 DELT--ETC(U)
APR 77 M A KWOK, J M HERBELIN, N COHEN F04701-76-C-0077
UNCLASSIFIED TR-0077(2940)-6 SAMSO-TR-77-73 NL

| OF |
ADA
039263

END

DATE
FILMED
5-77

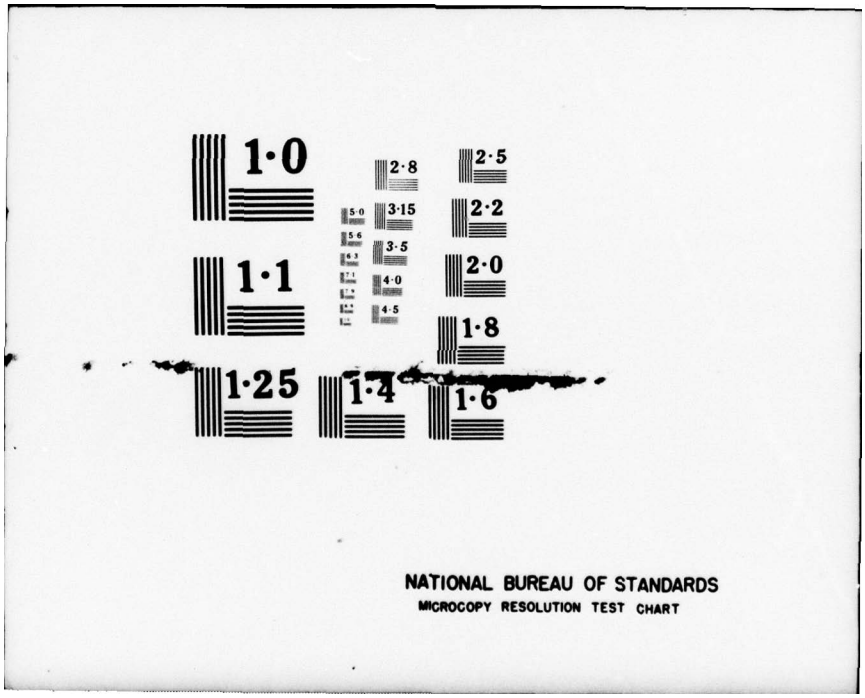
1·0
1·1
1·25
1·4
1·6
1·8
2·0
2·2
2·5
2·8
3·15
3·5
4·0
4·5
5·0
5·6
6·3
7·1
NATIONAL BUREAU OF STANDARDS
MICROCOPY RESOLUTION TEST CHART

REPORT SAMSO-TR-77-73

Collisional Quenching and Radiative Decay Studies of $NF(a^1\Delta)$ and $NF(b^1\Sigma^+)$

Aerophysics Laboratory
The Ivan A. Getting Laboratories
The Aerospace Corporation
El Segundo, Calif. 90245

15 April 1977

Interim Report

Prepared for

SPACE AND MISSILE SYSTEMS ORGANIZATION
AIR FORCE SYSTEMS COMMAND
Los Angeles Air Force Station
P.O. Box 92960, Worldway Postal Center
Los Angeles, Calif. 90009

This interim report was submitted by The Aerospace Corporation, El Segundo, CA 90245, under Contract No. F04701-76-C-0077 with the Space and Missile Systems Organization, Deputy for Advanced Space Programs, P. O. Box 92960, Worldway Postal Center, Los Angeles, CA 90009. It was reviewed and approved for The Aerospace Corporation by W. R. Warren, Jr., Director, Aerophysics Laboratory. Lieutenant A. G. Fernandez, SAMSO/YAPT, was the project officer for Advanced Space Programs.

This report has been reviewed by the Information Office (OI) and is releasable to the National Technical Information Service (NTIS). At NTIS, it will be available to the general public, including foreign nations.

This technical report has been reviewed and is approved for publication.

ARTURO G. FERNANDEZ, Lt, USAF
Project Officer

JOSEPH GASSMANN, Maj, USAF

FOR THE COMMANDER

FLOYD R. STUART, Colonel, USAF
Deputy for Advanced Space Programs

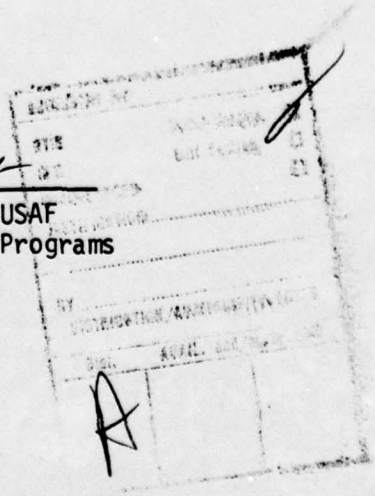

UNCLASSIFIED

SECURITY CLASSIFICATION OF THIS PAGE (When Data Entered)

REPORT DOCUMENTATION PAGE		READ INSTRUCTIONS BEFORE COMPLETING FORM
1. REPORT NUMBER SAMSO-TR-77-73	2. GOVT ACCESSION NO.	3. RECIPIENT'S CATALOG NUMBER
4. TITLE (and Subtitle) COLLISIONAL QUENCHING AND RADIATIVE DECAY STUDIES OF NF($a^1\Delta$) AND NF($b^1\Sigma^+$)		5. TYPE OF REPORT & PERIOD COVERED Interim rept.
		6. PERFORMING ORG. REPORT NUMBER TR-0077(2940)-6
7. AUTHOR(s) Munson A. Kwok, John M. Herbelin and Norman Cohen		8. CONTRACT OR GRANT NUMBER(s) F04701-76-C-0077
9. PERFORMING ORGANIZATION NAME AND ADDRESS The Aerospace Corporation El Segundo, Calif. 90245		10. PROGRAM ELEMENT, PROJECT, TASK AREA & WORK UNIT NUMBERS
11. CONTROLLING OFFICE NAME AND ADDRESS Space and Missile Systems Organization Air Force Systems Command Los Angeles, Calif. 90009		12. REPORT DATE 15 April 1977 13. NUMBER OF PAGES 28
14. MONITORING AGENCY NAME & ADDRESS (if different from Controlling Office) 30p.		15. SECURITY CLASS. (of this report) Unclassified 15a. DECLASSIFICATION/DOWNGRADING SCHEDULE

16. DISTRIBUTION STATEMENT (of this Report)

Approved for public release; distribution unlimited

17. DISTRIBUTION STATEMENT (of the abstract entered in Block 20, if different from Report)

18. SUPPLEMENTARY NOTES

19. KEY WORDS (Continue on reverse side if necessary and identify by block number)

Atomic and molecular physics	Flow tubes	Physical chemistry
Chemical kinetics	NF($a^1\Delta$)	Rate constants
Chemical lasers	NF($b^1\Sigma$)	
Chemically reactive flows	NF chemical kinetics	
Energy distribution and transfer	NF molecules	

20. ABSTRACT (Continue on reverse side if necessary and identify by block number)

Excited NF species is produced by the reaction of discharge-produced NF_2 with H atoms in the medium-pressure large-diameter flow tube. The collisional quenching rate coefficients of NF($b^1\Sigma^+$) by HF(0), H_2(0), and H and of NF($a^1\Delta$) by HF(0) and D_2(0) are studied. The endothermic energy-transfer rate coefficient for the NF($b^1\Sigma^+$) + HF(0) → NF($a^1\Delta$) + HF(2) process is 1×10^{12} cm^3 mol^{-1} sec^{-1} at 298°K; the rate coefficient for H + NF($b^1\Sigma^+$) is 3×10^{12} cm^3 mol^{-1} sec^{-1}; the radiative decay of NF($b^1\Sigma^+$) is 67 sec^{-1}, which is ten times larger than previously reported. The effects of D on NF($a^1\Delta$) are discussed.

DD FORM (FACSIMILE) 1473

409367

UNCLASSIFIED

SECURITY CLASSIFICATION OF THIS PAGE (When Data Entered)

PREFACE

The authors thank R. F. Heidner for helpful discussion, R. H. Ueunten for experimental assistance, and C. Blessing for help in preparing the manuscript.

CONTENTS

FIGURES

TABLES

I. INTRODUCTION

Herbelin and Cohen,[1] in a kinetic study of the H/NF_2 system, found that the reaction of H, D, or CH_3 with NF_2 produces electronically excited $NF(a^1\Delta)$ instead of ground-state or other excited states of NF:

$$R + NF_2(^2B_1) \rightarrow RF + NF(a^1\Delta) \qquad (R = H,\ D,\ or\ CH_3) \qquad (R1)$$

They also found that the $NF(b^1\Sigma^+)$ state is principally produced from energy-transfer processes with $HF(v \geq 2)$ or with electronically excited O_2.

$$HF(v = 2) + NF(a^1\Delta) \rightarrow HF(v' = 0) + NF(b^1\Sigma^+) + 295\ cm^{-1} \qquad (R2)$$

$$O_2(a^1\Delta_g) + NF(a^1\Delta) \rightarrow O_2(X^3\Sigma_g) + NF(b^1\Sigma^+) + 427\ cm^{-1} \qquad (R3)$$

The failure of vibrationally excited DF to participate in a process analogous to that of Reaction (2) was the basis for concluding that near-resonance is required for substantial transfer.

From these preliminary studies, it was concluded that this system is a chemical electronic laser candidate.[2] Some of the crucial rate coefficients needed for evaluating the system quantitatively and for constructing a model must be measured to assess further this possibility. Among the rate coefficients reported here are that for Reaction (2) and those for the quenching of $NF(b^1\Sigma^+)$ by H and H_2. The radiative decay rate for $NF(b^1\Sigma^+)$ is estimated. The effects of HF(0), D_2, and D on $NF(a^1\Delta)$ are discussed.

II. EXPERIMENT

The excited NF species was produced by the reaction of H or D with NF_2 in the medium-pressure (1 Torr) large-diameter (10 cm), fast-flow (4500 cm sec^{-1}) tube facility (Fig. 1) previously described.[3-5] For these experiments, NF_3 was substituted for SF_6 in a mixture that was passed through an rf discharge. The plasma was an efficient producer of F atoms; however, $[NF_2]$ was less than 0.5% of $[NF_3]_o$. For NF quenching studies, small concentrations in the limiting reagent were desirable in order to minimize NF-NF_x reactions. F atoms were quantitatively converted to H or D by reaction with H_2 or D_2 injected into the flow by means of the movable stainless-steel spoke injector. Purified HF(0) was injected into the flow through the Monel injector by means of a scheme previously described.[3] The O_2, NO, N_2, or N_2O was injected by means of a centerline quartz injector located at the rear of the flow tube. The injector passed beyond the discharge sidearm but was still 20 tube diameters from the optical system to ensure complete mixing.

Studies of the removal of NF by H or D required two additional experiments to establish the atomic concentrations. The spatial variation of H in the axial coordinate Z was determined by the injection of purified NO and by the observation of the 763-nm band emission of HNO, which was formed by the

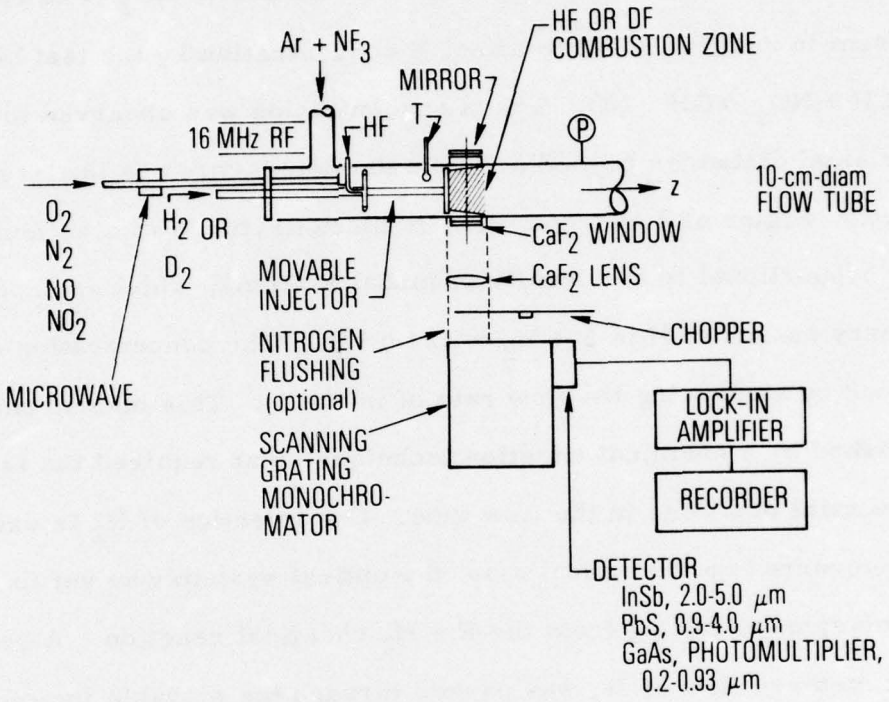

Fig. 1. Simplified experimental schematic

three-body recombination[5,6] of H + NO. The NO was purified to eliminate NO_2 by passage through a Cu trap at 195°K. Sufficient NO_2 (5 to 10%) was present in unpurified NO to affect H concentration by the fast bimolecular reaction $H + NO_2 \rightarrow OH + NO$. The H concentration was observed to be uniform for axial distances beyond 6.5 tube diameters after an initial mixing and reaction region of 2 to 4 cm. The H concentration was also found to be directly proportional to the density of initial F atoms, which is expected if the primary source of H is $F + H_2 \rightarrow HF(v) + H$. The concentration of H was determined by measuring the flow rate of initial F. This measurement was accomplished by a chemical titration technique[4] that required the injection of H_2 at two axial positions in the flow tube. One injection of H_2 in excess of initial F occurred on the optical axis; the optical system was set to observe HF(2) emissions resulting from the $F + H_2$ chemical reaction. A second carefully metered flow of H_2 was passed through the movable injector at an upstream position. The metered H_2 was systematically increased so that a total quenching point of HF(2) emissions could be determined. The flowrate of metered H_2 at this point is equal to the flowrate of initial F at the upstream position.

The method of determining collisional rate coefficients is successful when the NF excited state is not coupled to other NF states. The variation of number density averaged across tube diameter as a function of Z was measured. The sensitivity of the negative decay slope to varying chaperone density was extracted from a ln(N) versus Z plot. Such a dependence of the

absolute value of the decay slope S has been applied to HF(v) V-V and V-R transfer studies.[3,4] For the NF($b^1\Sigma^+$) state, S is written

$$S = \frac{1}{U'}\left[A_b + \sum_M k_M [M] + \frac{C}{p}\right] \qquad (1)$$

where U′ is the effective tube gas velocity, taken to be 1.6 times tube average gas velocity[7], A_b is the radiative decay rate, $k_M(M)$ is the quenching rate by chaperone M, and Cp^{-1} is the inverse pressure dependence caused by transverse diffusion effects and subsequent wall loss. Normally, the last term is not important in the determination of k_M since the quantity dS/d(M) is observed. However, in an estimate of the radiative decay rate, where all [M] is extrapolated to zero, Cp^{-1} must be known. In the cases of quenching by HF(0), a nearly resonant energy transfer is involved; therefore, the size of the reverse pumping rate term must be examined.

$$k_M[M][NF(b^1\Sigma^+)] >> k'_M[M^*][NF(a^1\Delta)] \qquad (2)$$

is required for a successful determination of k_M in the generalized energy-transfer reaction:

$$NF(b^1\Sigma^+) + M \underset{k_M}{\overset{k'_M}{\rightleftharpoons}} NF(a^1\Delta) + M^* \qquad (R4)$$

III. SPECTROSCOPY

Spontaneous emissions of from 250 to 3000 nm were observed. The signals used as diagnostics are listed in Table 1. The 0-0 band spectra of the $NF(b^1\Sigma^+)$ - $NF(X^3\Sigma^-)$ transitions centered at 528.8 nm and the $NF(a^1\Delta)$ - $NF(X^3\Sigma^-)$ transitions at 874.2 nm are the most important. Because the Q_P, Q_Q, and Q_R branches are narrow,[8, 9] individual vibrational rotational transitions were not resolved. Well over 80% of the spectrum at 298°K was observed to be within these branches. The empirical widths of the three overlapping Q-branches are estimated from the works of Jones to be 0.2 nm for the (b-X) and 0.5 nm for the (a-X) bands. The 874.2-nm band can overlap with the strong HF 3-0 vibrational-rotational overtone band at 880.0 nm from HF(3) produced in the reaction of F + H_2. Much of the study of $NF(a^1\Delta)$ therefore was performed with HF(3) adequately quenched or with D_2 used as the fuel. A series of strong bands in the 600- to 900-nm region was identified as the N_2 first-positive series ($B^3\Pi_g$ - $A^3\Sigma_u^+$). Vibrational fundamentals of that series interfered at 874 nm. Since $N(^2D)$ atoms had been shown[1] to be the precursor of $N_2(B^3\Pi_g)$, they were removed[14, 15] for the $NF(a^1\Delta)$ studies by O_2, N_2O, or NO. It was found that the N_2 first-positive series did not vary its non-Boltzmann vibrational distribution with Z or with flow conditions; hence, an arbitrary (7-4) band was chosen for study (Table 1). As an indicator for HF(v) pumping of $NF(b^1\Sigma^+)$, HF(2) was followed by means of the P_{2-1} (4) line.

Table 1. Spectroscopy for $H + NF_2$ System

Transition	Center Wavelength, nm	Radiative Decay Rate, sec^{-1}	Reference
$NF(b^1\Sigma^+ - X^3\Sigma^-, 0\text{-}0)$	528.8	67[a]	8
$NF(a^1\Delta - X^3\Sigma^-, 0\text{-}0)$	874.6		1, 9
HF, $P_{3\rightarrow2}(3)$ line	2854.2	256	13
HF, $P_{2\rightarrow1}(4)$ line	2760.4	206	13
HF, $P_{1\rightarrow0}(1)$ line	2475.8	72	13
HF, $R_{3\rightarrow0}(1)$ line	874.0	0.49	13
$N_2(B^3\Pi_g - A^3\Sigma_u^+, 2\text{-}1)$	872.2		10
$N_2(B^3\Pi_g - A^3\Sigma_u^+, 7\text{-}4)$	634.0	5×10^4	10
$NH(A^3\Pi_i - X^3\Sigma^-, 0\text{-}0)$	336.0	2.2×10^6	11, 12

[a]Determined in this work.

Absolute intensity calibrations and radiative decay-rate numbers permitted the determination of absolute number densities, averaged along the tube diameter of most of the excited species. The instrument width of the optical system had been observed to be triangular and 4.2 nm wide for the deliberately low resolution studies conducted. Accordingly, it was assumed that the instrument width was much greater than the narrow empirical widths of these bands or isolated spectral lines. The total power P in photons observed from a band or line therefore is given by

$$P = (\eta A_o \Omega_o L) \frac{h\nu}{4\pi} AN \tag{3}$$

where $\eta A_o \Omega_o L$ are the transmission and geometric factors, ν is the band or line center wavelength, A is the radiative decay rate, and N is the number density of band or line averaged over the optical volume.

A strong narrow band emission located between 330 and 340 nm was reidentified as the $NH(A^3\Pi_i - X^3\Sigma^-)$ band centered at 336 nm[11,12] rather than $NF(A^3\Pi - X^3\Sigma^-)$ emission.[1] The strong sensitivity of the 336-nm emission to the variation of H_2 and a significant similarity of the axial variation to that of the N_2 first-positive emission were the bases for our conclusion.

IV. RESULTS AND DISCUSSION

The absolute number densities averaged along the tube diameter of various excited species were plotted for a typical run (Fig. 2). The H-atom Z plot follows the relative HNO intensity; the absolute peak concentration is set equal to initial F. The H-atom loss in 70 cm is small because the flow is sufficiently fast so that wall losses are minimal. The number density of $NF(b^1\Sigma^+)$ can be determined since its radiative decay rate has been deduced in this work.

However, only the photon flux, $A_a[NF(a^1\Delta)]$, can be estimated in Fig. 2 since a value for A_a cannot be resolved in this work. The Z plot, labelled H_2, is a deduction after both N_2 first-positive and HF $3 \rightarrow 0$ emissions are subtracted. The first-positive Z plot can be independently measured at the 634-nm band, HF(3), either at a $3 \rightarrow 0$ P-branch position or at $3 \rightarrow 2$ in the infrared. The curve labelled H_2-O_2 indicates that the first-positive emission is experimentally suppressed by removing N with O_2. The O_2 affects the $NF(a^1\Delta)$ density very little. Recent work[16] indicates that A_a may be $\sim 1.0\ sec^{-1}$. Then, in accordance with Equation (1), initial $[NF_2/F]$ is $\sim 0.5\%$.

Experimental rate coefficients k_M for the quenching of $NF(b^1\Sigma^+)$ or $NF(a^1\Delta)$ by M can be deduced from S versus [M] plots (Figs. 3-6). The k_M can be computed from Equation (1) when dS/dM and U′ ($\sim 6800\ cm\ sec^{-1}$) have been determined. For cases where nonzero dS/dM is actually observed, the estimated uncertainty on the coefficient is ±50% of the value at a 95% confidence level. In cases such as that shown in Fig. 5, an upper bound to k_M can be

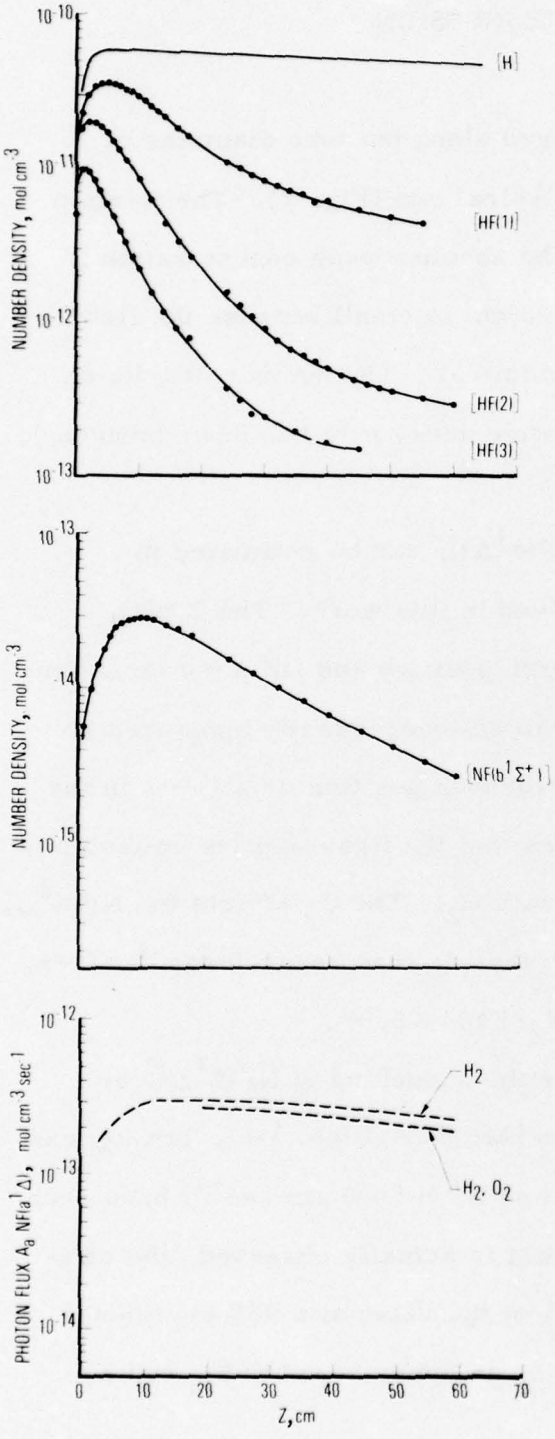

Fig. 2. Number densities averaged across tube diameter versus axis position Z for various product species in H + NF_2 reactive flow. Tube conditions: 1 Torr, 298°K. Molar flow rates = Ar, NF_3, and H_2 = 18375, 12, and 200 μmol sec^{-1}, respectively. U′ = 6800 cm sec^{-1}. When used, O_2 = 1000 μmol sec^{-1}.

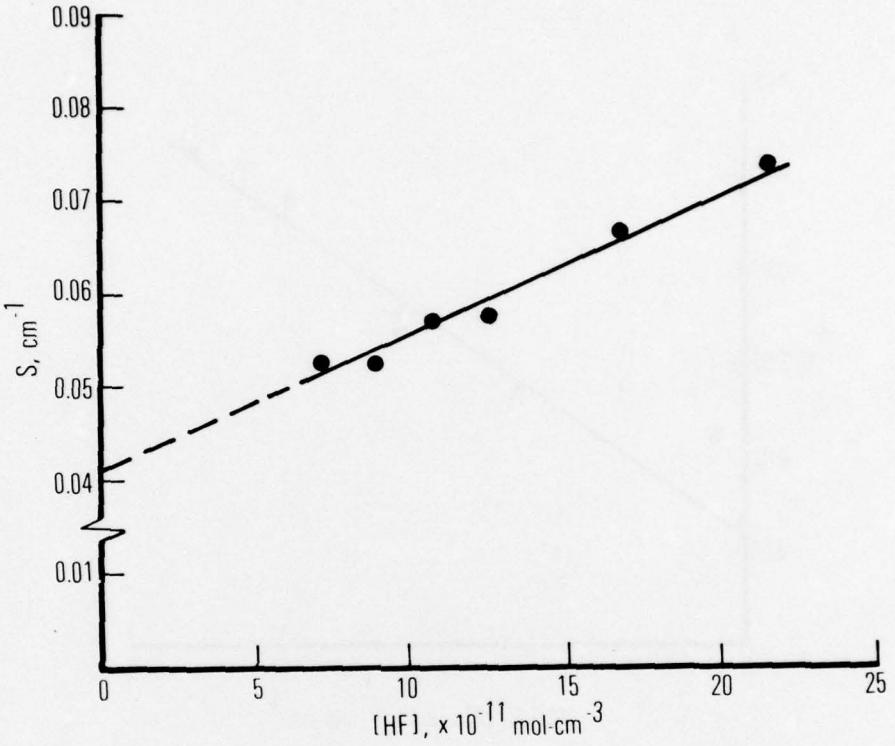

Fig. 3. $NF(b^1\Sigma^+)$ decay slope S versus HF concentration. Tube conditions: 1 Torr, 298°K. Molar flow rates of Ar, F, and H_2 = 18000, 23, and 200 μmol sec^{-1}, respectively. U′ = 6800 cm sec^{-1}.

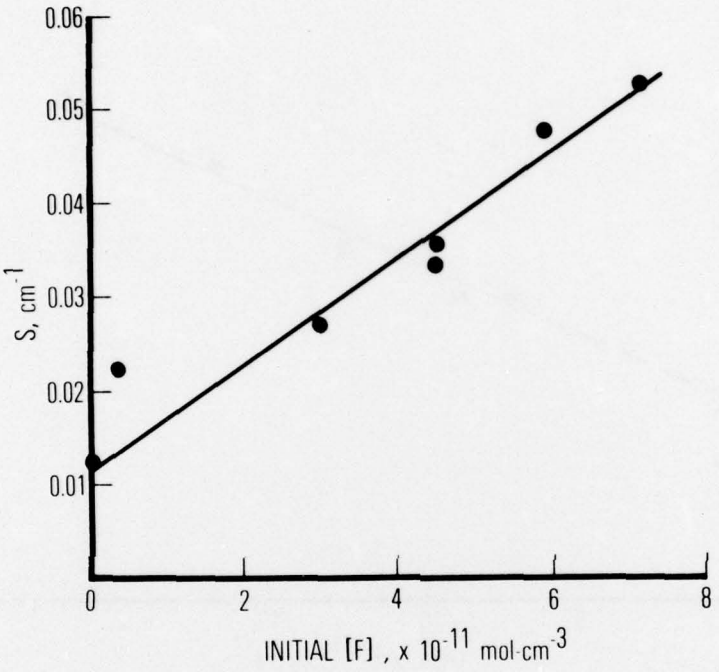

Fig. 4. $NF(b^1\Sigma^+)$ decay slope S versus initial F-atom concentration. Tube concentrations: 1 Torr, 298°K. Molar flow rates of Ar, and H_2 = 18000, and 200 μmol sec^{-1}, respectively. U′ = 6800 cm sec^{-1}.

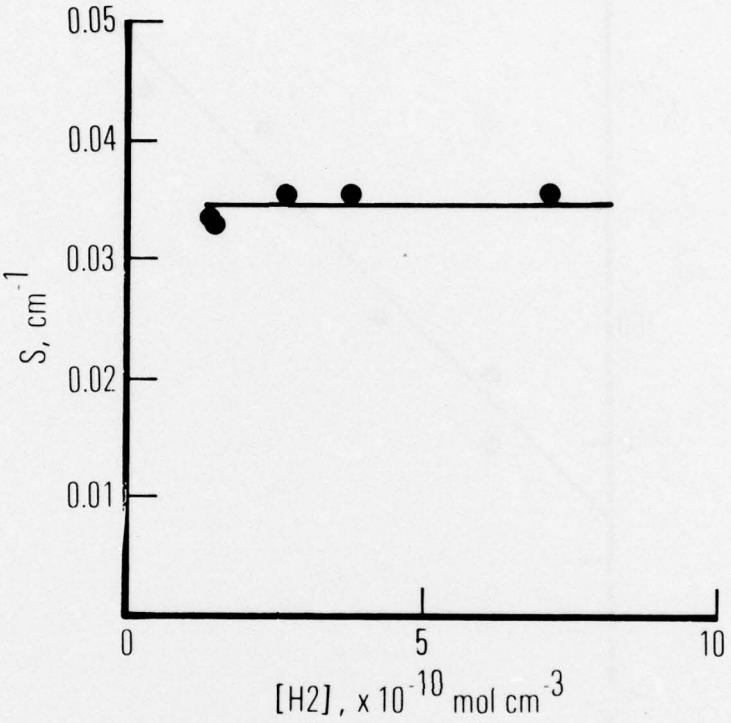

Fig. 5. NF($b^1\Sigma^+$) decay slope S versus H_2 concentration. Tube conditions as in Fig. 2.

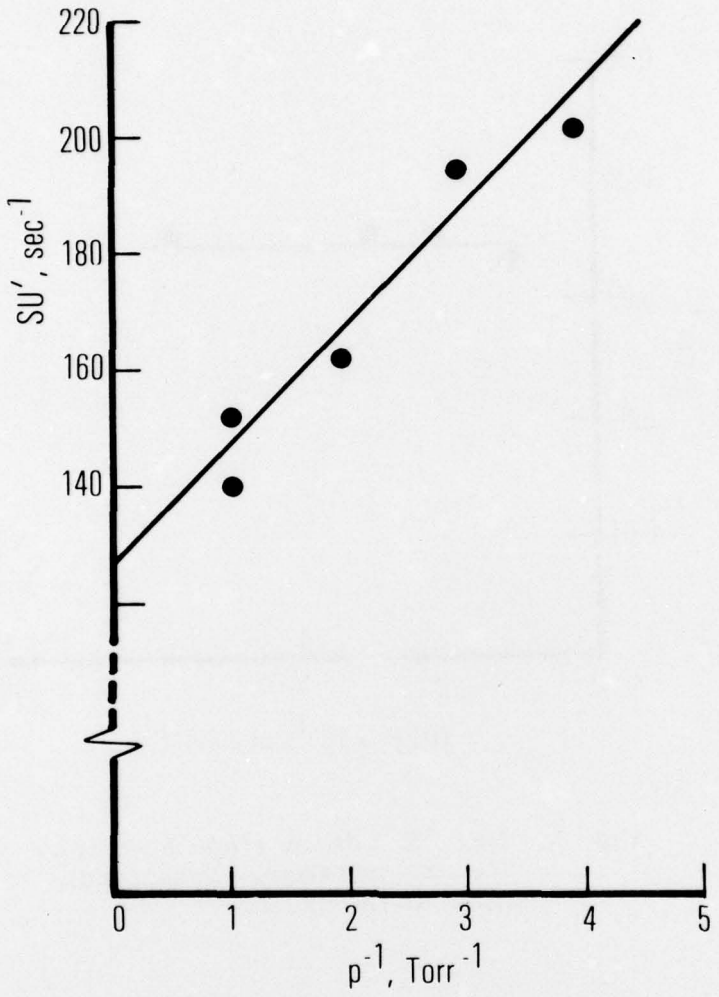

Fig. 6. Total decay rate SU′, sec^{-1}, of $NF(b^1\Sigma^+)$ versus inverse pressure. p^{-1} as in Fig. 1. NF_3, H_2, and initial F-atom flow rates = 12,200 and 20 μmol sec^{-1}.

given on the basis of the maximum density of M used. The maximum observable characteristic time in this flow tube is 50 msec.

A. $\underline{NF(b^1\Sigma^+) + HF}$

The HF quenching of $NF(b^1\Sigma^+)$ probably occurs through the transfer of internal energy in the molecules, Reaction (2), and not through an E-T transfer or reactive process. The energy defect of 295 cm^{-1} is computed with HF assumed to be in the J = 0 state and NF in v = 0 and J = 0 states. For the vibrational constants of $NF(a^1\Delta)$, which have not been reported, we take an average of those for $NF(b^1\Sigma^+)$ and $NF(X^3\Sigma^-)$. A comparison of ω_e values of the corresponding states of the isoelectronic O_2 states suggests that this is a good approximation for the $a^1\Delta$ state. From these considerations, a 30-cm^{-1} uncertainty in the energy defect is estimated. The resultant exothermic transfer rate at 298°K is then 4.5 times that of the endothermic rate in Reaction (2). Since $[NF(a^1\Delta)]$ appears to be 10 times $[NF(b^1\Sigma)]$, for Equation (2) to be properly satisfied, $[HF(0)]:[HF(2)] > 45$. The principal production of HF(2) in this system is from the reaction $F + H_2$; for the highest flow rates of HF(0), typically, $[HF(0)]:[HF(2)] > 200$ in the region of $NF(b^1\Sigma^+)$ decay ($Z > 25$ cm in Fig. 2). In addition, with increasing HF(0) injected, the strong $HF(v > 1) + HF$ self-quenching[3] tends to lower the $HF(v > 0)$ densities below those depicted in Fig. 2. That the E-T and reactive processes are slow, compared to the E-V mechanism, is evidenced by the very low upper bound for the rate of $HF(0) + NF(a^1\Delta)$.

B. $NF(b^1\Sigma^+) + H$

Quenching of $NF(b^1\Sigma^+)$ by H atoms was studied by varying the initial F-atom flow. Atomic hydrogen and HF flows equal the initial F flow because of the dominant reaction $F + H_2 \rightarrow H + HF$. The decay slopes are shown in Fig. 4. $[H] >> [NF(a^1\Delta)]$ is virtually invariant in Z for 65 cm (Fig. 2). As shown in Fig. 2, $[HF(v \geq 2)]$ has a sharp maximum on an intermediate flow-tube time scale Z, which permits pumping of $NF(b^1\Sigma^+)$, but has minimal interference with the NF decay slope. In this decay region, most of product HF is in the ground vibrational level, with concentration equal to [H]. The collisional quenching rate coefficient deduced from $dS/d[F]$ is then the sum of quenching coefficients from H and HF. Subtraction of the already determined k_{HF} yields k_H. Almost certainly, $H + NF(b^1\Sigma^+)$ is a reactive mechanism, but the fate of products is not clearly defined since either HF or HN could be generated.

The value of k_H deduced is considered an upper bound in the sense that other $NF(b^1\Sigma^+)$ quenchers can be generated in the discharge and downstream in a manner correlated with initial F. Such species might be N_2, N, and $NF(X^3\Sigma^-)$. Since nitrogen in large amounts did not affect the observed excited NF species, and the production of $N(^4S)$ by the microwave discharge did not appear to change the $NF(b^1\Sigma^+)$ decay slope qualitatively, $NF(X^3\Sigma^-)$ is the most likely contaminant quencher. The concentration of discharge-produced $NF(X^3\Sigma^-)$ should be, at most, of the same order as initial $[NF_2]$. Therefore, the maximum density of NF(X) is $< 10^{-13}$ mol cm^{-3} or < 1% [H]. A 0.1 gaskinetic rate then does not affect k_H. In this fuel-rich H/NF_2 system, $N(^2D)$ atoms, which scaled with initial F, probably were produced[1] by H + NF.

$[N(^2D)]$ was limited by NF and NF_2 to ~0.5% [H]. Subsequent reactions of $N(^2D)$ with NF or H_2 can produce such species as N_2 or NH with the same upper bound densities of 0.5% H. A one-tenth gaskinetic quenching effect by $N(^2D)$ or NH on $HF(b^1\Sigma^+)$ would lower k_H by 5%.[14, 15]

C. NF($b^1\Sigma^+$) Radiative Decay

The zero F-atom intercept deduced by the least-squares straight-line fit in Fig. 4 can give an estimate of $NF(b^1\Sigma^+)$ radiative decay rate. The limit of zero [F] was approached by systematically lowering NF_3 and rf power; these variations effectively removed the quenching effects of H and HF and the possible side effects of N_2, N, and NF from the intercept. The effects of fixed ultrapure H_2 and Ar remained. Quenching by H_2 was negligible (Table 2 and Fig. 5). As shown in Fig. 6, Ar mainly determined the rate of transverse diffusion of $NF(b^1\Sigma^+)$ to the wall. The fitted straight line of SU′ versus p^{-1} indicated that at 1 Torr there was a 20-sec^{-1} effective diffusion decay rate. The line in Fig. 4 yielded an intercept of 77 sec^{-1}, from which [Reaction (2)] 20 sec^{-1}, as a result diffusion, was subtracted. The total radiative decay rate of $NF(b^1\Sigma^+, v = 0)$, A_b, remained. Most of A_b was attributed to the 528.8-nm $b^1\Sigma^+ \rightarrow X^3\Sigma$ transition. The radiation was assumed to be electric dipole-like since it was a strong observable intercombination band.[8] A hypothetical $NF(b^1\Sigma^+ \rightarrow a^1\Delta)$ band would demand violation of the strong singlet-singlet angular momentum selection rule $\Lambda = 0, \pm 1$. Therefore, this radiation could be described by no stronger than an electric quadrupole and should be orders of magnitude weaker. Since only the Q_P, Q_Q, and Q_R, branches were followed, it was assumed, of course, that rotational equilibrium exists in the NF states as well as in HF.

Table 2. Collisional Quenching Rate Coefficients

Excited Species	M	$k_{M'}$ $cm^3\ mol^{-1}\ sec^{-1}$
$NF(b^1\Sigma^+)$	HF	1×10^{12}
$NF(a^1\Delta)$	H	3×10^{12}
	H_2	$<4 \times 10^{10}$
	HF	$<10^{11}$
	D_2	$<4 \times 10^{10}$

Experiments for other studies can be used to verify the observed A_b. From HF + NF($b^1\Sigma^+$) quenching studies, the contributions of fixed H (or discharge products) and diffusion must be subtracted from the ordinate intercept (Fig. 3); from Ar variations (Fig. 6), the decay rates of H and HF. An average value of A_b was deduced to be 67 ± 30 sec^{-1} (Table 3). This value is an order of magnitude larger than that reported by Clyne and White.[17] Their smaller value suggests a pumping mechanism independent of N_2, but the lack of details concerning their experiment prevents further comment.

D. NF($a^1\Delta$) + M

With HF or D_2 as collision partners, no variation in S with [M], much like Fig. 5, was obtained; therefore, only upper-bound rate coefficients could be computed. If there is an E-V transfer for NF($a^1\Delta$) + HF(0), it probably results in the formation of HF(3); this exothermic (by 66 cm^{-1}) process is the most nearly resonant one possible. The two-quantum transfer is probably exothermic by 3690 cm^{-1}; if the rotational energy of HF is involved very much, this effective defect can be reduced. That these transfers were much less favorable than that of Reaction (2) is probably the result of the requirement of conservation of electron spin in NF, which necessitates a spin flip here but not in the transfer described by Reaction (2). The comparative effects of HF(0) on NF($a^1\Delta$) and NF($b^1\Sigma^+$) are indications that the NF molecule obeys spin conservation in such collisions.[1,2] Furthermore, the highly resonant transfer requires a three-quantum jump in HF, which should be less probable than a two-quantum process.

Table 3. Radiative Decay Rate of $NF(b^1\Sigma^+)$

System	Initial [F], μmol sec^{-1}	Intercept, sec^{-1}	A_b, sec^{-1}
$H + NF(b^1\Sigma^+)$ quenching	--	77	57 ± 30
Diffusion (Fig. 6)	20	120	72 ± 35
$HF + NF(b^1\Sigma^+)$ quenching	24	287	69 ± 35
Average A_b			67 ± 30

The quenching of $NF(a^1\Delta)$ by D atoms was observed to occur with a rate coefficient of $<10^{12}$ cm^3 mol^{-1} sec^{-1}. There is greater uncertainty in this number than in that for H + $NF(b^1\Sigma^+)$ because the study was made in the presence of O_2. Two additional reactions had to be considered: the reactions D + O_2 and $N(^2D)$ + O_2. The former can be dismissed because it is endothermic by 17 kcal/mole.[18] The products of the fast reaction[14] (N^2D) + O_2 → O + NO scaled with initial [F]; the maximum possible concentrations of O and NO were limited by NF or NF_2 to about 0.5% [H]. Either O + $NF(a^1\Delta)$ or NO + $NF(a^1\Delta)$ can affect substantially the conclusion if either rate coefficient is gaskinetic. However, an O + NF reaction probability of 0.1 per collision has been reported,[17] and large amounts of NO do not appear to alter the decay slopes in the present experiments.

V. CLOSURE

Related work is given in a published abstract.[19] Work in determining rate coefficients for Reactions (1) and (3) is continuing.

REFERENCES

1. J. M. Herbelin and N. Cohen, Chem. Phys. Lett. 20, (1973).
2. J. M. Herbelin, unpublished work.
3. M. A. Kwok and R. L. Wilkins, J. Chem. Phys. 63 2534 (1975).
4. M. A. Kwok and N. Cohen, J. Chem. Phys. 61, 5221 (1974).
5. M. A. Kwok and R. L. Wilkins, J. Chem. Phys. 60, 2189 (1974).
6. M. A. A. Clyne and B. A. Thrush, Discuss. Faraday Soc. 33, 139 (1962).
7. R. V. Poirier and R. W. Carr, J. Phys. Chem. 75, 1593 (1971).
8. A. E. Douglas and W. E. Jones, Can. J. Phys. 44, 2251 (1966).
9. W. E. Jones, Can. J. Phys. 45, 21 (1967).
10. M. Jeunehomme, J. Chem. Phys. 45, 1805 (1966).
11. R. N. Dixon, Can. J. Phys. 37, 1171 (1959).
12. W. H. Smith and H. S. Liszt, J. Quantum Spectroscopy Radiative Transfer 11, 45 (1971).
13. J. M. Herbelin and G. Emanuel, J. Chem. Phys. 60, 689 (1974).
14. C. L. Lin and F. Kaufman, J. Chem. Phys. 55, 3760 (1971)
15. G. Black, T. G. Slanger, G. A. St. John, and R. A. Young, J. Chem. Phys. 51, 116 (1969).
16. J. M. Herbelin, M. A. Kwok, N. Cohen, unpublished work.
17. M. A. A. Clyne and I. F. White, Chem. Phys. Lett. 6, 465 (1970).
18. W. Wilson, J. Phys. and Chem. Ref. Data 1, 535 (1972).
19. M. A. Kwok, J. M. Herbelin, and N. Cohen, in Proceedings of Second Annual Colloquium on Electronic Transition Lasers, ed. J. Steinfeld, MIT Press, Cambridge, Massachusetts, 1976, pp. 8-12.

THE IVAN A. GETTING LABORATORIES

The Laboratory Operations of The Aerospace Corporation is conducting experimental and theoretical investigations necessary for the evaluation and application of scientific advances to new military concepts and systems. Versatility and flexibility have been developed to a high degree by the laboratory personnel in dealing with the many problems encountered in the nation's rapidly developing space and missile systems. Expertise in the latest scientific developments is vital to the accomplishment of tasks related to these problems. The laboratories that contribute to this research are:

Aerophysics Laboratory: Launch and reentry aerodynamics, heat transfer, reentry physics, chemical kinetics, structural mechanics, flight dynamics, atmospheric pollution, and high-power gas lasers.

Chemistry and Physics Laboratory: Atmospheric reactions and atmospheric optics, chemical reactions in polluted atmospheres, chemical reactions of excited species in rocket plumes, chemical thermodynamics, plasma and laser-induced reactions, laser chemistry, propulsion chemistry, space vacuum and radiation effects on materials, lubrication and surface phenomena, photosensitive materials and sensors, high precision laser ranging, and the application of physics and chemistry to problems of law *enforcement* and biomedicine.

Electronics Research Laboratory: Electromagnetic theory, devices, and propagation phenomena, including plasma electromagnetics; quantum electronics, lasers, and electro-optics; communication sciences, applied electronics, semiconducting, superconducting, and crystal device physics, optical and acoustical imaging; atmospheric pollution; millimeter wave and far-infrared technology.

Materials Sciences Laboratory: Development of new materials; metal matrix composites and new forms of carbon; test and evaluation of graphite and ceramics in reentry; spacecraft materials and electronic components in nuclear weapons environment; application of fracture mechanics to stress corrosion and fatigue-induced fractures in structural metals.

Space Sciences Laboratory: Atmospheric and ionospheric physics, radiation from the atmosphere, density and composition of the atmosphere, aurorae and airglow; magnetospheric physics, cosmic rays, generation and propagation of plasma waves in the magnetosphere; solar physics, studies of solar magnetic fields; space astronomy, x-ray astronomy; the effects of nuclear explosions, magnetic storms, and solar activity on the earth's atmosphere, ionosphere, and magnetosphere; the effects of optical, electromagnetic, and particulate radiations in space on space systems.

THE AEROSPACE CORPORATION
El Segundo, California